

RESEARCH PAPER

## Introducing a Polypyrrole (PPy)-Manganese Ferrite ( $MnFe_2O_4$ ) Nanocomposite Based Microwave Absorber for Studying the Effect of the Radiation on the Modification of the Patient's Functional State

Felix A. Pyatakovich <sup>1\*</sup>, Olga V. Mevsha <sup>1</sup>, Tatyana I. Yakunchenko <sup>1</sup>, Kristina F. Makkonen <sup>1</sup>, Viktor M. Uvarov <sup>2</sup>

<sup>1</sup> Belgorod State University, 85, Pobedy St., Belgorod, 308015, Russia

<sup>2</sup> Gubkin Branch of the "Belgorod State Technological University named after V.G. Shukhov". 15-a, Dzerzhinsky St., Gubkin, 309186, Russia.

### ARTICLE INFO

#### Article History:

Received 17 November 2021

Accepted 19 February 2022

Published 01 April 2022

#### Keywords:

Alpha spindle model

Microwave radiation

$MnFe_2O_4$

Nanomaterials absorber

Super-low intensity

### ABSTRACT

In the present work, polypyrrole (PPy)-manganese ferrite ( $MnFe_2O_4$ ) nanocomposite based microwave absorber for studying the effect of the radiation on the modification of the patient's functional state is reported. X-ray powder diffraction (XRPD), Fourier transform infrared spectroscopy (FTIR) and scanning electron microscope (SEM) images are used to characterize the prepared nanocomposites. Recently, new microwave-based imaging and hyperthermia applications have emerged in the field of diagnostics and therapy. This technology involves the application of low power microwaves, utilising contrast between the relative permittivity of tissues to identify pathologies. This contrast can be further enhanced through the implementation of nanomaterials. For therapy, this technology can be applied in tissues either through hyperthermia. Nanomaterials can absorb electromagnetic radiation and can enhance the microwave hyperthermic effect. Microwave generators of super-low intensity in the centimeter wavelength range at a power level not exceeding  $1 \mu W/cm^2$  have been successfully used in experimental and clinical medicine. In the present work, we have implemented a project aimed at the development of a modular-type technical system designed to generate microwave radiation with specified properties. This article presented the electrophysiological efficiency of super-low intensity radiation in the centimeter range of wavelengths modulated by low-frequency signals similar to the EEG rhythm with cyclical variability of the duty cycle.

### How to cite this article

Pyatakovich F A, Mevsha O V, Yakunchenko T I, Makkonen K F, Uvarov V M. Introducing a Polypyrrole (PPy)-Manganese Ferrite ( $MnFe_2O_4$ ) Nanocomposite Based Microwave Absorber for Studying the Effect of the Radiation on the Modification of the Patient's Functional State. J Nanostruct, 2022; 12(2):245-253. DOI: 10.22052/JNS.2022.02.003

### INTRODUCTION

Spinel-type ferrites such have been used as conventional microwave absorption materials. However, spinel-type ferrites show Snoek's limit,

and the magnetic loss decreases drastically at several gigahertz. Manganese ferrite ( $MnFe_2O_4$ ) is a common spinel ferrite material and has been widely used in microwave and magnetic

\* Corresponding Author Email: [fr.education90@yahoo.com](mailto:fr.education90@yahoo.com)



recording applications. Recently, it has been shown that magnetic nanocomposites are useful as microwave-absorbing materials due to their advantages in respect to light weight, low cost, design flexibility, and microwave properties over pure ferrites [1-5]. Nanomaterials that respond to electromagnetic (EM) radiation have been suggested for either imaging and/or hyperthermia. These nanomaterials need to be suitably biocompatible as well as able to interact with EM energy to induce a signal response or increase the temperature locally. To this end, various nanomaterials have been suggested as contrast agents in microwave (MW) imaging, with the aim to increase contrast between the target and background tissue [6-11].

Non-thermal radiation power produced in a huge number of extremely high frequency (EHF) devices with frequencies is  $\leq 10$  mW. Such a frequency range at such a radiation power belongs to the so-called absorption resonances, since it is completely absorbed at the surface layer of skin, does not penetrate either directly to healthy or pathological tissues of a particular organ, and only affects acupuncture points and biological channels [12]. The effects of millimeter therapy on the functional state of the patient under stress have been revealed [13]. The positive results in the treatment of cerebral circulation disorders using millimeter waves have been investigated [14,15]. In the last decade, in practical medicine, equipment has been used that emits super-low intensity centimeter waves at a power level not exceeding 1  $\mu\text{W}/\text{cm}^2$  [16]. For such electromagnetic radiation, the aquatic environment of the body becomes radio-transparent [17], which makes it possible

to place the radiator antenna of the device directly on the projection of one or another organ [18]. The purpose of the research is to optimize the methods of super-low intensity microwave action with the development of the structure of specialized deterministic modulation models and control algorithms designed for the directed transformation of EEG patterns with subsequent modification of the patient's functional state. According to the above mentioned explanation, the aims of the present study are development of a structure for a prototype super-low intensity generator of centimeter waves with a frequency of 1000 MHz and an output radiation power of 1 microwatt, description of the deterministic models of relaxation patterns in the form of an alpha rhythm spindle, including the basic pattern of the structure, the pattern of modulating impulses and the temporal pattern of the modulating signals, and research on the adequacy of the developed models to real electrophysiological processes of the brain.

The modulating impulse pattern is 1 wave of theta rhythm + a spindle of 4 waves of alpha rhythm. 1 impulse with a frequency of 4 Hz + 4 impulses with a frequency of 10 Hz. The time pattern of the modulating signals consisted of impulse durations and pause durations: [1 \* (0.23 + 0.02) + 4 \* (0.08 + 0.02)]. The parameters of the optimization model for the control of modulated action in the form of an alpha-rhythm spindle are considered in Table 1.

## MATERIALS AND METHODS

### Materials and Instrumentals

Chemicals including metal salts,

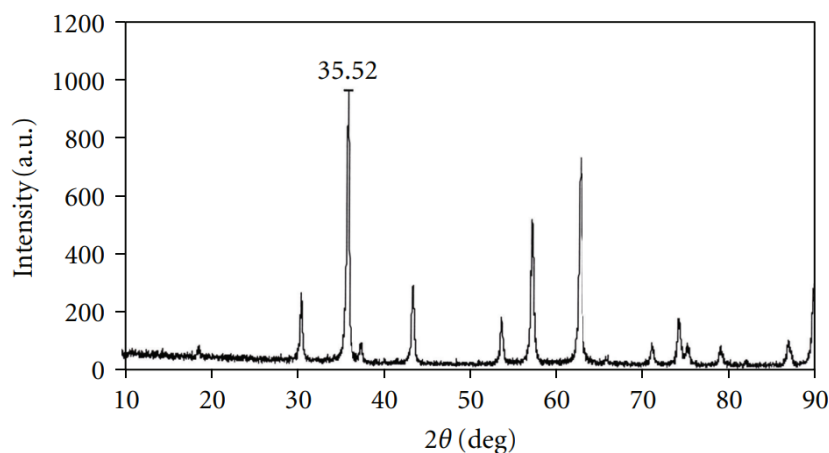


Fig. 1. X-ray diffraction for MnFe<sub>2</sub>O<sub>4</sub> nanoparticles.

hexamethylenetetramine (HMTA), potassium persulfate (KPS), and ethylene glycol (EG) are analytical grade (Merck) and were used without further purification. Water was deionized, doubly distilled, and deoxygenated prior to use. Styrene and methacrylic acid (analytical grade, Merck) were distilled to remove the inhibitor. Pyrrole monomer (analytical grade, Merck) was distilled twice under reduced pressure. DBSA and acrylic resin were of industrial grade. The other reagent, including iron chloride (FeCl<sub>3</sub>), was of analytical grade (Merck). The morphology of coated particles and nanocomposite was observed by scanning electron microscopy (SEM) with a JSM-6301F (Japan) instrument operated at an accelerating voltage of 10 kV. X-ray powder diffraction (XRD) patterns of the nanoparticles assemblies were collected on a PhilipsPW 1800 with Cu-K radiation

under CuK $\alpha$  radiation ( $\lambda = 1.5406\text{\AA}$ ).

## RESULTS AND DISCUSSIONS

### X-Ray Diffraction

Fig. 1 shows the XRD pattern of manganese ferrites. It can be clearly noted from Figure 1 that the ferrite shell are phase-pure spinel structure in all cases according to the standard XRD patterns of MgFe<sub>2</sub>O<sub>4</sub> ( $2\theta = 30.1, 33.0, 35.5, 43.7, 53.2, 57.0, 62.4, 74.0, 71.0, 78.0, 86.5$ ).

Fig. 2 presents SEM images of MgFe<sub>2</sub>O<sub>4</sub> nanoparticles and polypyrrole-MgFe<sub>2</sub>O<sub>4</sub> nanocomposites. The images show that compositing MgFe<sub>2</sub>O<sub>4</sub> with the organic agent increases the particle size of the final product.

As shown in Fig. 3, the characteristic peaks of PPy-manganese ferrite nanocomposite occur at 2920, 1555, 1461, 1313, 1188, 1038, 1006, 959, 908, 670, 576, 2311, and 2920 cm<sup>-1</sup>.

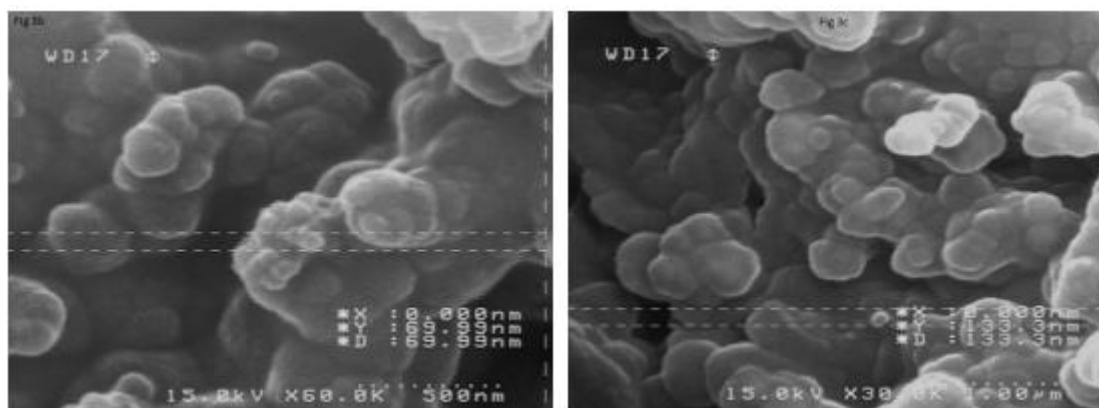


Fig. 2. SEM images of MgFe<sub>2</sub>O<sub>4</sub> (left) and polypyrrole-MgFe<sub>2</sub>O<sub>4</sub> nanocomposite (right).

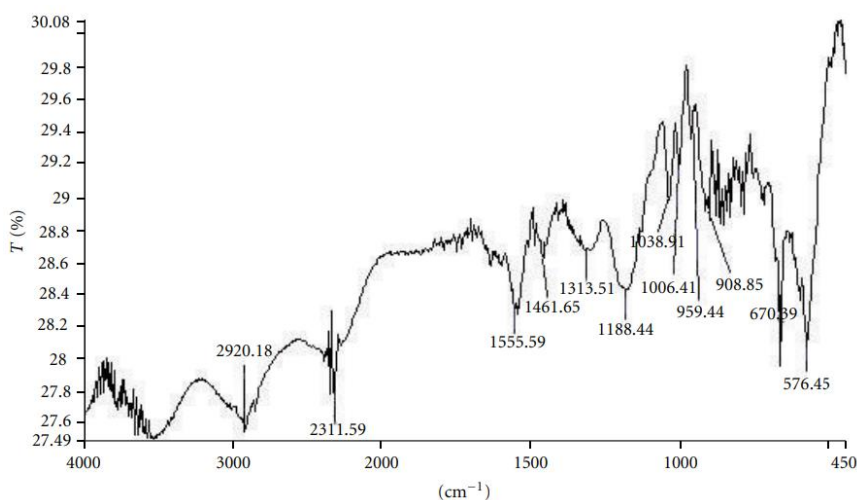


Fig. 3. FTIR spectra of polypyrrole - MgFe<sub>2</sub>O<sub>4</sub> nanocomposite.

908, 670, and 576 cm<sup>-1</sup>. The peaks at 1555 and 1461 cm<sup>-1</sup> are attributed to the characteristic C=C and C-N stretching of polypyrrole ring; the peaks at 1313 and 1188 cm<sup>-1</sup> correspond to N-H bending and asymmetric C-N stretching modes of the PPy ring, respectively. The peak around 1038 cm<sup>-1</sup> is associated with vibrational modes of N=Q=N (Q refers to the quinonic type rings), indicating that PPy is formed in our sample. The peaks at 2920 and 1038 cm<sup>-1</sup> attributed to C-H aliphatic stretching vibration and the symmetric and antisymmetric stretching vibration of SO<sub>3</sub> group of dopant (DBSA), respectively. The peaks at 1006–908 cm<sup>-1</sup> are attributed to the p-disubstituted aromatic ring C-H out-of-plane bending. However, the characteristic peaks of MnFe<sub>2</sub>O<sub>4</sub> for F-O and Mn-O stretching vibrations can be observed at wave numbers 670 and 576 cm<sup>-1</sup>.

For currents above 0.3 mA, two peaks with Lorentzian line shape were observed for each current as shown in Fig. 4. The lower-frequency peak may be attributed to a centre precession mode while the higher-frequency peak probably arises from a mode with large amplitude at the sides of the nanopillar. Quantitative data are gathered in Fig. 5, where we report the frequencies, powers, and linewidths of the centre precession mode as a function of applied current. First, a blueshift in the oscillation frequencies with increasing the d.c.

current is observed. For 0.5 mA ≤ d.c. ≤ 1.5 mA, the frequencies increase rapidly, resulting in a current modulation capability of 0.22 GHz/mA. Further increasing current, the frequencies exhibit a slight increase. The similar trend has been also observed in other systems, which suggests that the steady-state excitation corresponds to an out-of-plane precession. Second, the integrated power of the centre mode increases gradually with increasing the d.c. current and reaches 5 nW at d.c. = 4 mA. Fig. 6. Presents schematic diagram of the proposed all-optical microwave oscillator.

From Table 1 it follows that the filling factor of the EEG modulation signals has the form of a crescendo-decrescendo: 50% -80% -70% -60% -50%. That is, the intensity of the impact gradually increases for 1.8 seconds and then gradually decreases within 2.0 seconds. It is easy to see that the inhalation-exhalation cycle is simulated by the time parameters. The total implementation time is 3.8 seconds. Therefore, if the formula is repeated 79 times, the total implementation time will be approximately 300 seconds or 5 minutes. By repeating the exposure formula 237 times, the realization time is 900 seconds or 15 minutes.

Further, studies were carried out on the adequacy of the developed models of exposure to microwave radiation to real electrophysiological processes of the brain. As you know, the stability

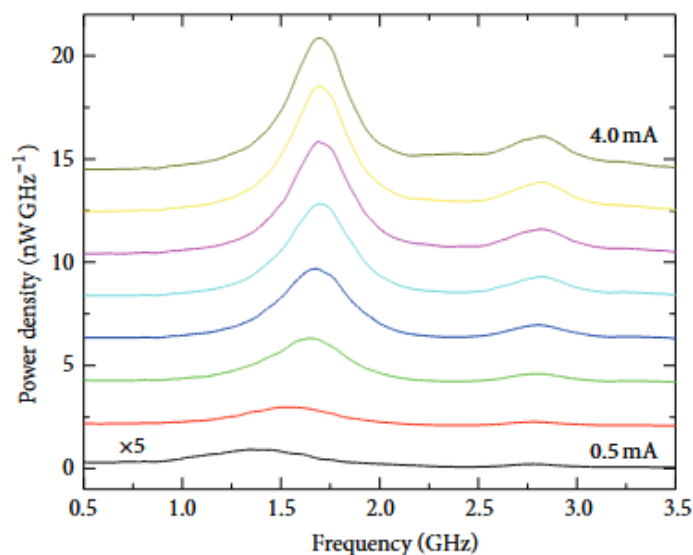


Fig. 4. Current-induced magnetoresistance oscillations for one representative device for positive current between 0.5  $\mu$ A and 4  $\mu$ A with 0.5  $\mu$ A steps at zero magnetic field. A vertical offset of 2 nW/GHz is applied to the curves for visual clarity.

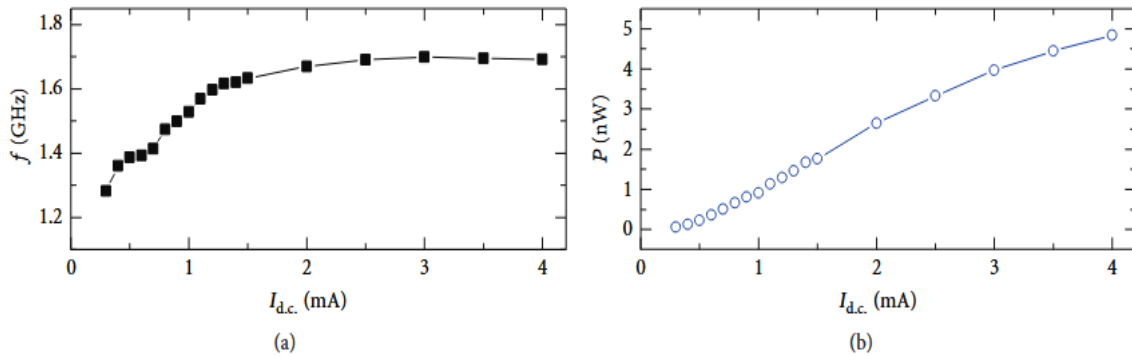


Fig. 5. (a) Frequency and (b) integrated power as a function of applied current.

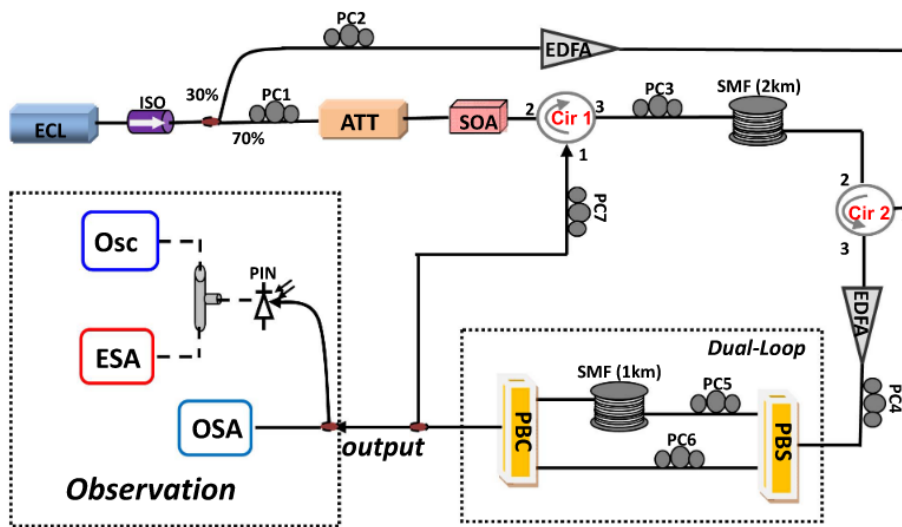


Fig. 6. Schematic diagram of the proposed all-optical microwave oscillator. ECL, external cavity laser; ISO, isolator; PC, polarization controller; ATT, attenuator; SOA, semiconductor optical amplifier; Cir, circulator; EDFA, erbium-doped fiber amplifier; PBS, polarization beam splitter; PBC, polarization beam combiner; Osc, oscilloscope; ESA, electrical spectrum analyzer; OSA, optical spectrum analyzer.

$\theta\alpha$  of the nucleus of the electroencephalogram pattern of a healthy person is determined by a highly probabilistic relationship between  $\theta$  and  $\alpha$  rhythm. Moreover, the ratio of alpha and theta rhythms depends on the adaptive mechanisms and determines the level of plasticity of the neurodynamic activity of the brain. With an excitable type of neurosis, the frequency spectrum of the EEG contains a theta-beta nucleus, and with an inhibitory type of neurosis, theta nucleus. Patients with increased emotional instability, irritability, hot temper require correction of the functional state by transforming the existing pathological EEG pattern. In this case, as a rule, an increase in alpha activity and its connections with theta components is required [19]. In the course of

clinical trials, the emitter of modulated super-low-intensity microwave oscillations with a power of 1 mKW was installed on the occipital fosse region. The duration of the irradiation was 30 minutes.

In the period before and after the exposure, the electroencephalogram of the left and right hemispheres of the brain was recorded using a special system "BOSLAB". This biotechnical system with an EEG training module was manufactured by Komsib, Novosibirsk. Registration certificate № 2011/11236. 12. 07. 2011. The recording of the electroencephalogram was carried out in order to assess the level of neurodynamic activity of the brain in the period before and after the modulated microwave impact.

For clinical studies, patients with type II

Table 1. Deterministic alpha spindle model of EEG signals.

EEG rhythm	Frequency Hz	Impact period		Number of ticks	Filling factor %	Realization Time (s)
		Impulse time	Pause time			
alpha	10	0.05	0.05	8	50	0.8
alpha	10	0.08	0.02	10	80	1.0
alpha	10	0.07	0.03	10	70	1.0
alpha	10	0.06	0.04	6	60	0.6
alpha	10	0.05	0.05	4	50	0.4
Total time						$\Sigma = 3.8$ s

diabetes mellitus were selected, hospitalized in the endocrinology department of the city clinical hospital No. 1. The selection was carried out by a selective method of research. The criteria for inclusion in the study were: 1. Type 2 diabetes mellitus with concomitant pathology in the form of essential hypertension II and coronary heart disease, including obese patients with metabolic syndrome. 2. Women aged 40 and over. 3. Agreement on participation in research.

A total of 90 women were examined and treated. All patients were from the same social group, aged 40–65 years. Most of the women were employed, of which 91% were employees of enterprises and organizations. Most of the patients had higher or incomplete higher education (70%). The results obtained were evaluated from the standpoint of the success and effectiveness of super-low intensity modulated microwave impact. At the same time, changes in the structure of the EEG pattern and quantitative indicators of plasticity of neurodynamic processes in the brain were taken into account on the basis of neural network research methods<sup>8; 9; 10</sup>. So, for example, the lack of dynamics of quantitative indicators of the structure of EEG rhythms indicates an unsuccessful microwave action [20].

When receiving a positive result of the impact, for example, accompanied by an increase in the proportion of alpha activity and a decrease in the proportion of theta rhythm, the relationship that does not persist until the next period of the study was considered to be a successful result. In the presence of a positive dynamics of restructuring of EEG rhythms and its preservation after impact to the next examination period, it was customary

to consider this type as effective [21].

The recordings were made after the first day, after the fifth day and after the tenth day of action by means of modulated EEG with similar microwave signals. Unsuccessful, successful and effective dynamics of the EEG pattern in the process of super-low intensity microwave influence was assessed using circular EEG diagrams and their analytical calculations, in particular, the coefficients of plasticity of neurodynamic activity of the brain.

From the analyzed EEG dynamics, it follows that the modulated microwave impact in the group of patients with unsuccessful action does not lead to reliable rhythm shifts over 10 days of the study, since the plasticity of the neurodynamic activity of the brain, judging by the  $\alpha/\theta$  ratio, remained at a low level on all days of the study: 0.88; 0.83; 1.17. The nonparametric criterion of Fisher's angular transformation in the range of the alpha rhythm indicated the absence of reliable differences ( $p > 0.05$ ). Patients with successful EEG correction showed a significant increase in the proportion of the alpha rhythm ( $p < 0.05$ ) and a decrease in the proportion of theta rhythm. A gradual increase in the level of plasticity of the neurodynamic activity of the brain after each subsequent session is revealed, namely: 0.70; 1.70; 2.70. In the interval between actions, a low level of plasticity of neurodynamic activity of the brain remains: 0.75; 1.17; 1.14. Consequently, such results can be considered successful, but not effective, that is, they do not lead to changes in the patient's functional status. Finally, in the third group of patients, the dynamics of the restructuring of the EEG pattern, judging by the coefficient of plasticity,

after super-low intensity modulated microwave impact from session to session (in session 3) increased: 1.77; 2.26; 2.95.

Attention is also drawn to the dynamics of the EEG pattern restructuring in the period before impact: 1.39; 2.04; 2.08, which remained at a high level until the next treatment session.

This group of patients also showed clinical signs of correction of the functional state: irritability decreased, mood improved, sleep was restored. Therefore, this type of correction of neurodynamic activity of the brain with positive clinical dynamics should be considered as effective.

Summarizing, the above presented material should be noted that super-low-intensity microwave radiation, modulated by low-frequency EEG-like signals, provides a restructuring of the patient's pathological EEG pattern due to the transformation of the structure of the neurodynamic processes of the brain. The modification of the functional state of the patient is carried out through changes in the intrasystemic mechanisms of regulation. The duration of the preservation of the transformed EEG pattern depends on the initial level of plasticity of the pathological EEG pattern: the higher the level of plasticity, the earlier it is observed, the transformation of the EEG pattern and for a longer time, its new structure will be preserved. It is especially important to note that the revealed facts of the positive effect of super-low intensity modulated centimeter radiation on

the normalization of the neurodynamic activity of the brain can be used for the drug-free primary prevention of disorders of the neurodynamic activity of the brain in patients with functional disorders in the form of various neuroses: neurasthenia, psychasthenia and hysteria. The results of a comparative analysis of the Spielberger test values are presented in Table 2.

From the data presented in Table 2, it follows that in patients with an effective result of impact, the total level of low and moderate situational anxiety is 90%, and in patients with a successful result - 63%. This difference is statistically reliable.

Patients with an ineffective result in half of the cases have a low and moderate level and in half of the cases a high level of situational anxiety. It should be emphasized that the difference in the level of situational anxiety in patients with an unsuccessful result and in patients with a successful result is reliable only for a one-sided test. This means that in patients with a successful result, the proportion of patients with a moderate level of situational anxiety is reliably higher than the proportion of patients with an unsuccessful result in this range. In patients with unsuccessful results, the proportion of patients with a high level of situational anxiety is reliably higher.

Thus, by summarizing the results of the studies obtained on the analysis of the Spielberger test, we can conclude that with an effective result of modulated EEG by such microwave signals, along

Table 2. Dynamics of indicators of situational anxiety using the Spielberger test under the influence of modulated super-low intensity microwave radiation

The level of situational anxiety in points	Impact result			Difference modulus		
	Ineffective	Successful	Effective			
	P1%	P2%	P3%	P1- P2	P1-P3	P2-P3
Low ≤30	17	18	30	1	13	12
Moderate 31–45	33	45	60	12	27	15
High ≥ 46	50	37	10	13	40	27
Total	100	100	100	26	80	54
D (Xi)	-	-	-	13%	40%	27%
Significance of differences	-	-	-	p<0.05	p<0.05	p<0.05

with the transformation of the EEG pattern, a modification of the functional state of patients is also noted. The quantitative parameters of the indicators of such a modification in patients with effective results reliably higher those in patients with only successful results. The dynamics of a decrease in signs of psycho emotional stress begins to appear only after 4-5 procedures of modulated microwave impact: sleep improves, irritability decreases, anxiety decreases. The positive dynamics stabilizes only by the 10th session of effect. Models of frequency modulation of a carrier therapeutic signal of super-low-intensity of 1 microwatt with a frequency of 1 GHz by reference signals of an electroencephalogram reflecting neurodynamic relaxation processes have been developed. On the basis of structural models of theta alpha activity of the EEG, digital analogs of the optimization of the effect were formed by changing the duty cycle of the modulating signal by varying the impulse duration and the pause duration. The software microcode for controlling the modulated microwave action included a cycle of 3.8 second step-by-step changes in the duty cycle of low-frequency signals in the alpha spindle structure with the values: 50% -70% -80% -70% -60%.

## CONCLUSION

In the present study, we have successfully fabricated nanoscale STOs by colloidal lithography and optical lithography instead of the expensive e-beam lithography. The fabricated STO device showed microwave signal generation under d.c. current. The generated microwave signal can be controlled by adjusting the d.c. current or magnetic field. Besides, the clinical studies showed that the selected codified models of EEG patterns designed to modulate super-low intensity carrier microwave signals, as well as the algorithms for controlling the optimization of the treatment procedure, implemented on their basis, are adequate to real electrophysiological processes of the brain, since they provide the expected results. The super-low intensity microwave radiation provided correction of the patient's functional state, both due to changes in the intrasystemic mechanisms of regulation (modification of neurodynamic processes in the brain), and by influencing the intersystem levels of regulation (normalization of the adrenergic status) through changes of the cyclical duration of pulse intervals and respiratory

act.

## CONFLICT OF INTEREST

The authors declare that there is no conflict of interests regarding the publication of this manuscript.

## REFERENCE

1. Birsöz B, Baykal A, Sözeri H, Toprak MS. Synthesis and characterization of polypyrrole-BaFe<sub>2</sub>O<sub>4</sub> nanocomposite. *J Alloys Compd.* 2010;493(1-2):481-485.
2. Giannakopoulou T, Kompotiatis L, Kontogeorgakos A, Kordas G. Microwave behavior of ferrites prepared via sol-gel method. *J Magn Magn Mater.* 2002;246(3):360-365.
3. Sugimoto S, Haga K, Kagotani T, Inomata K. Microwave absorption properties of Ba M-type ferrite prepared by a modified coprecipitation method. *J Magn Magn Mater.* 2005;290-291:1188-1191.
4. Tabatabaie F, Fathi MH, Saatchi A, Ghasemi A. Microwave absorption properties of Mn- and Ti-doped strontium hexaferrite. *J Alloys Compd.* 2009;470(1-2):332-335.
5. Xiao H-M, Liu X-M, Fu S-Y. Synthesis, magnetic and microwave absorbing properties of core-shell structured MnFe<sub>2</sub>O<sub>4</sub>/TiO<sub>2</sub> nanocomposites. *Composites Science and Technology.* 2006;66(13):2003-2008.
6. Slavin A, Tiberkevich V. Nonlinear Auto-Oscillator Theory of Microwave Generation by Spin-Polarized Current. *IEEE Trans Magn.* 2009;45(4):1875-1918.
7. Zeng Z, Finocchio G, Jiang H. Spin transfer nano-oscillators. *Nanoscale.* 2013;5(6):2219.
8. Slonczewski JC. Current-driven excitation of magnetic multilayers. *J Magn Magn Mater.* 1996;159(1-2):L1-L7.
9. Berger L. Emission of spin waves by a magnetic multilayer traversed by a current. *Physical Review B.* 1996;54(13):9353-9358.
10. Kiselev SI, Sankey JC, Krivorotov IN, Emlay NC, Schoelkopf RJ, Buhrman RA, et al. Microwave oscillations of a nanomagnet driven by a spin-polarized current. *Nature.* 2003;425(6956):380-383.
11. Rippard W, Pufall M, Kaka S, Silva T, Russek S. Current-driven microwave dynamics in magnetic point contacts as a function of applied field angle. *Physical Review B.* 2004;70(10).
12. Repin AN, Lebedeva EV, Gorokhov AS, Nonka TG, Sergienko TN. Primenenie medikamentoznoy zashchity mozga na rannem etape rehabilitatsii pri operatsii koronarnogo shuntirovaniya u bol'nykh s ishemicheskoy boleznyu serdtsa. *CardioSomatics.* 2015;6(1-1):83-84.
13. Gazizov RM, Atsel EA, Khaliullina GA, Volchkova NS, Klimova NA. Vliyaniye rozuvastatina na dinamiku lipidnogo spektra i sostoyaniye immunnogo sistema u bol'nykh ishemicheskoy boleznyu serdtsa. *CardioSomatics.* 2013;4(1-1):20-21.
14. Osipov IB, Lebedev DA, Komissarov MI, Osipov AI, Aleshin IY, Safroshina EV. Maloinvazivnoe lechenie obstruktivnogo megauretera. *Urologicheskie vedomosti.* 2015;5(1):71.
15. Isaeva NV, Prokopenko SV, Rodikov MV, Abroskina MV, Ondar VS, Subocheva SA, et al. Stiff-person syndrome: a clinical observation. *Zhurnal nevrologii i psikiatrii im SS Korsakova.* 2019;119(6):96.
16. Pyatakovich F.A., Mevsha O.V., Yakunchenko T.I., Makkonen K.F. Translyacionny'e issledovaniya v processe

- razrabotki biotekhnicheskoy sistemy` sverxnizko intensivnoj decimetrovoj terapii// Nauchny`e trudy` VIII-go Mezhdunarodnogo kongressa «Slaby`e i sverxslaby`e polya i izlucheniya v biologii i medicine». SPb, 2018. 8:182.
17. Petrosyan, V.I., Sinicyn, N.I., Elkin, V. A., Majborodin, A.V., Tupikin, V.D., Kreniczkiy, A.P., Nadezhkin, Yu.M., Problemy` pryamogo i kosvennogo nablyudeniya rezonansnoj prozrachnosti vodny`x sred v millimetrovom diapazone // Biomedicinskaya radioelektronika , 2000. 1: 34-40.
  18. Pyatakovich F.A., Mevsha O.V., Yakunchenko, T.I., Makkonen K.F., Personificirovannaya sverxnizko intensivnaya DMV–terapiya u bol`ny`x saxarny`m diabetom II tipa. // Kurortnaya medicina, 2018. 3:70-72.
  19. Pyatakovich, F., Khlivnenko, L., Yakunchenko, T., Makkonen, K., Mevsha, O., Translational methods for solving the tasks of the project to develop bioengineering system and the neuronet processes of diagnostic// Proceedings Allergy, Asthma, Copd, Immunophysiology & Norehabilitology: Innovative Technologies. Editor Professor Revaz Sepiashvili., E-book: 289-296. Filodiritto International Proceedings. Printed by Rabbi S.r.l., Via del Chiù, 74, Bologna (Italy). 2017.
  20. Pyatakovich, Felix A., Khlivnenko, Lubov V., Yakunchenko, Tatyana I., Makkonen, Kristina F., Mevsha, Olga V., Development of an algorithm for automatic clustering of atypical autoregressive clouds of inter-pulse intervals by means of using a self-organizing artificial neural network. J Adv Res Dyn Con Sys, 2018. 10: 1853-1857, 10 -Special Issue.
  21. Pyatakovich, Felix A., Mevsha, Olga V., Yakunchenko, Tatiana I., Makkonen, Kristina F., Biotechnical system of automatic classification scattergrams and evaluation of atrial fibrillation outcomes. International Journal of Pharmacy & Technology (IJPT) 2016. 8 (2):14129-14136.